

MULTI-MODAL MULTI-PATTERN PUSHOVER ANALYSIS FOR SEISMIC DESIGN OF SPATIAL FRAMES

Makoto Ohsaki¹⁾, Atsushi Uchida²⁾ and Jingyao Zhang³⁾

1) Associate Professor, Kyoto University, Kyoto, Japan

2) Graduate Student, Kyoto University, Kyoto, Japan

3) Post-doctoral Research Fellow, Kyoto University, Kyoto, Japan

ABSTRACT

A new approach is presented for determination of equivalent static seismic loads for evaluating maximum seismic responses of spatial frames. The responses are estimated by series of pushover analyses considering possible phase differences in the dominant modes. The vibration modes of the initial elastic structure are used, and the damping due to plastic dissipation is modeled by equivalent linearization for inelastic systems. The accuracy of the proposed method is demonstrated in the numerical examples of an arch-type long-span truss and a 3-story 3-dimensional building frame.

1. INTRODUCTION

In seismic design process of structures, static analysis is commonly adopted to approximately estimate the maximum responses. For this purpose, there have been numerous studies on development of equivalent static loads for building frames considering effect of several dominant modes, usually in the form of modal combination. For inelastic systems, however, the modal combination rules for elastic systems are not directly applicable. Therefore, several methods for adaptive force distribution are proposed to follow more closely the time-variant distributions of inertia forces, so as to provide better prediction [1, 2]. Modal combination rules are also presented for defining the static loads [3, 4]. Kunnath [5] presented a method to take snapshots of the deformation at which a response quantity has the maximum value. However, an empirically estimated combinations of modal coefficients are used for defining several load patterns.

In these methods for building structures, the base shear and roof displacement are used as representative force and displacement, which cannot be used for estimating the vertical responses of spatial frames. Nakazawa *et al.* [6] presented a method of adaptive modal pushover analysis for spatial frames. Kato *et al.* [7] applied multi-modal pushover analysis to reticulated domes. In this study, we present a general approach to define several load patterns using the elastic eigenmodes and response spectra. A new definition is proposed for the representative displacement and acceleration that is applicable to spatial frames. The variation of the maximum responses are successfully evaluated by static pushover analyses of several times.

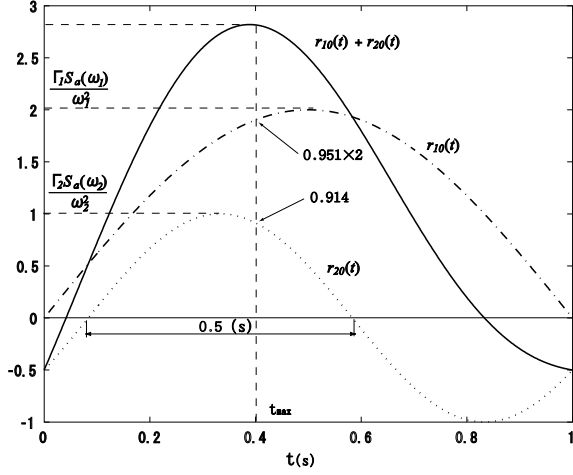


Fig.1. Determination of coefficients α_n for the case where two modes dominate.

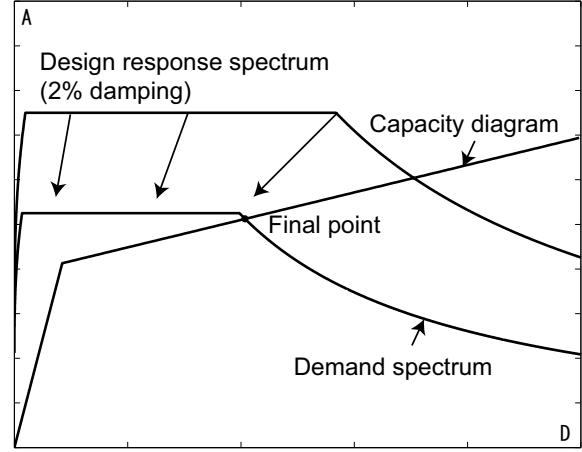


Fig.2. Capacity diagram and demand spectrum.

2. MODAL LOAD COEFFICIENTS

Let Φ_n denote the n th mode of undamped free vibration. The vector in which the components corresponding to the input direction are 1, and the remaining components are 0 is denoted by \mathbf{I} . The participation factor Γ_n and the equivalent mass M_n of the n th mode are defined as

$$\Gamma_n = \Phi_n^T \mathbf{M} \mathbf{I}, \quad M_n = (\Gamma_n)^2 \quad (1)$$

where \mathbf{M} is the mass matrix, and Φ_n is orthonormalized by $\Phi_i^T \mathbf{M} \Phi_j = \delta_{ij}$ with the Kronecker delta δ_{ij} . Let \mathbf{f}_{n0} denote the static load vector corresponding to the n th mode. We assume, for simplicity, that N modes from 1st to N th are used. The static seismic load \mathbf{f}_0 is defined as a linear combination of \mathbf{f}_{n0} with the coefficient α_n as

$$\mathbf{f}_0 = \sum_{n=1}^N \alpha_n \mathbf{f}_{n0} = \sum_{n=1}^N \alpha_n \Gamma_n S_a(\omega_n) \mathbf{M} \Phi_n \quad (2)$$

where $S_a(\omega_n)$ is the value of the acceleration response spectrum $S_a(\omega)$ corresponding to the n th mode, and ω_n is the n th natural circular frequency.

If damping is not very large, the deformation at which a displacement component takes the maximum can be found by applying the inertia forces \mathbf{f}_0 in Eq. (2) statically to obtain the maximum displacement. Therefore, the process of finding the maximum displacement is reduced to that of determining the coefficients α_n for the seismic load vector. Suppose the component of mode n makes a sinusoidal response in full scale around the time instance of maximum response of a particular displacement component. Then the response $r_{n0}(t)$ of the n th mode with the amplitude $\Gamma_n S_a(\omega_n) / \omega_n^2$ and the phase angle θ_n is given as

$$r_{n0}(t) = \frac{\Gamma_n S_a(\omega_n)}{\omega_n^2} \sin(\omega_n t - \theta_n) \quad (3)$$

Suppose θ_n is distributed randomly in the interval $[0, 2\pi]$, and consider the case where the maximum response is to be found for the i th displacement component. Then define the sum $r_0(t)$ of

$r_{n0}(t)$ as

$$r_0(t) = \sum_{n=1}^N \text{sign}(\phi_{ni}) r_{n0}(t) \quad (4)$$

where $\text{sign}(\phi_{ni})$ is the sign of the i th component of Φ_n . Let t_{\max} denote the time at which $r_0(t)$ takes the maximum absolute value. Then the coefficient α_n at t_{\max} is adopted as the load coefficient:

$$\alpha_n = \sin(\omega_n t_{\max} - \theta_n) \quad (5)$$

where the maximum value is computed in the half period of the most dominant mode.

For example, suppose the modes 1 and 2 dominate, and we find the coefficients α_1 and α_2 as illustrated in Fig. 1. The amplitudes of the two modes are assumed as $\Gamma_1 S_a(\omega_1)/\omega_1^2 = 2.0$, $\Gamma_2 S_a(\omega_2)/\omega_2^2 = 1.0$. The natural periods are $2\pi/\omega_1 = 2.0$ sec. and $2\pi/\omega_2 = 1.0$ sec., and the phase angles are $\theta_1 = 0$ and $\theta_2 = \pi/6$. As is seen, $r_{10}(t) + r_{20}(t)$ takes the maximum value at $t = t_{\max} = 0.4$ sec., and the corresponding load coefficients are obtained as $\alpha_1 = 0.951$ and $\alpha_2 = 0.914$. Several load patterns can be obtained by assigning several values of θ_2 . If the i th components ϕ_{1i} and ϕ_{2i} of the two modes have the same sign, t_{\max} is defined as the time at which $r_{10}(t) + r_{20}(t)$ has the maximum value. However, if ϕ_{1i} and ϕ_{2i} have different signs, $r_{10}(t) - r_{20}(t)$ is to be maximized. It is desired to rigorously consider the magnitudes of ϕ_{1i} and ϕ_{2i} ; however, only the signs are considered to reduce the necessary number of patterns.

3. ESTIMATION OF INELASTIC RESPONSE BY EQUIVALENT LINEARIZATION

In most of the methods for evaluation of inelastic responses of building frames, the roof displacement and base shear are used as the representative displacement and force. However, for spatial frames, vertical displacements and forces sometimes dominate over the horizontal ones; hence, other representative displacement and acceleration should be defined.

Let \mathbf{u}^i and \mathbf{a}^i denote the vectors of displacements and accelerations at the i th step of the pushover analysis, where \mathbf{a}^i is obtained by dividing the nodal force by the corresponding nodal mass. The vectors \mathbf{u}^i and \mathbf{a}^i are decomposed to the mode components as

$$\mathbf{u}^i = \sum_{n=1}^N c_{un}^i \Phi_n, \quad \mathbf{a}^i = \sum_{n=1}^N c_{an}^i \Phi_n \quad (6)$$

where c_{un}^i and c_{an}^i are the coefficients for the i th mode that are obtained as

$$c_{un}^i = \Phi_n^T \mathbf{M} \mathbf{u}^i, \quad c_{an}^i = \Phi_n^T \mathbf{M} \mathbf{a}^i \quad (7)$$

Denoting by D_n^i and A_n^i the modal displacement and acceleration at the i th step of pushover analysis, \mathbf{u}^i and \mathbf{a}^i are written as

$$\mathbf{u}^i = \sum_{n=1}^N \Gamma_n D_n^i \Phi_n, \quad \mathbf{a}^i = \sum_{n=1}^N \Gamma_n A_n^i \Phi_n \quad (8)$$

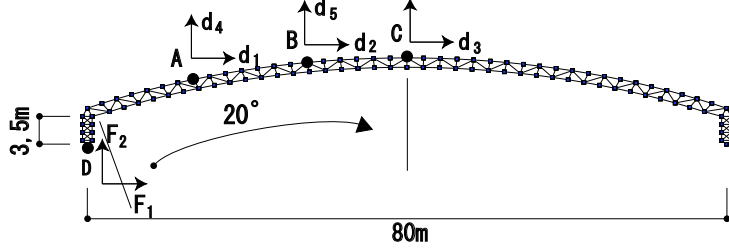


Fig.3. An arch model.

From Eqs.(6)–(8), the displacement and acceleration of the n th mode are obtained as

$$D_n^i = \frac{c_{un}^i}{\Phi_n^T \mathbf{M} \mathbf{I}}, \quad A_n^i = \frac{c_{an}^i}{\Phi_n^T \mathbf{M} \mathbf{I}} \quad (9)$$

Hence, considering the orthogonality of modal responses, the representative displacement, acceleration, and the equivalent period at step i of pushover analysis are obtained as

$$D^i = \sqrt{\sum_{n=1}^N (D_n^i)^2}, \quad A^i = \sqrt{\sum_{n=1}^N (A_n^i)^2}, \quad T_{eq} = 2\pi \sqrt{\frac{D^i}{A^i}} \quad (10)$$

The energy dissipation due to plastification is considered using the technique of equivalent linearization. Pushover curve between D^i and A^i are approximated by a bilinear relation with the displacement D_y and acceleration A_y when the first plastification occurs. Let D_u and A_u , respectively, denote the values of D^i and A^i at the intersection point. The equivalent damping coefficient h_{eq} is defined using the plasticity factor $\mu = D_u/D_y$ as

$$h_{eq} = h_0 + \kappa h_{eq}^p = h + \kappa \frac{2(\mu - 1)(1 - \gamma)}{\pi\mu(1 + \gamma\mu - \gamma)} \quad (11)$$

where h_0 is the initial damping coefficient, h_{eq}^p is the equivalent damping coefficient due to plastification, and γ is the stiffness after yielding. The parameter κ is the damping modification factor in ATC-40 [10], which is defined for Types A, B, and C depending on the ductility of the structure. The target spectrum is the design acceleration response spectrum for 5% damping specified by Notification 1461 of the Ministry of Land, Infrastructure and Transport (MLIT), Japan, corresponding to the performance level of life safety. The amplification factor for the ground of 2nd rank and the definition of the spectrum reduction factor due to damping in Notification 1457 of MLIT are used.

The inelastic responses are evaluated as follows using the capacity spectrum approach [8] as illustrated in Fig. 2:

- Step 1:** Carry out pushover analysis for each static load pattern to generate the history of D^i and A^i from Eq. (10). Determine the yield point (D_y, A_y) to obtain the bilinear relation.
- Step 2:** Compute the demand diagram A^R at all steps.
- Step 3:** Find the intersection point that has the smallest difference between A^i and A^R to obtain the maximum response.



Fig.4. Eigenmodes of the arch-type truss.

Table 1. Load coefficients for Pattern 1 (maximize $r_{10}(t) + r_{30}(t)$).

	P1-1	P1-2	P1-3	P1-4	P1-5	P1-6	P1-7	P1-8
α_1	0.83	0.86	0.88	0.92	0.95	0.98	0.99	1.00
α_3	0.26	0.49	0.70	0.77	0.84	0.90	0.98	1.00

Table 2. Load coefficients for Pattern 2 (maximize $r_{10}(t) - r_{30}(t)$).

	P2-1	P2-2	P2-3	P2-4	P2-5	P2-6	P2-7	P2-8
α_1	1.00	1.00	0.99	0.97	0.94	0.92	0.88	0.86
α_3	-1.00	-0.98	-0.95	-0.91	-0.85	-0.69	-0.61	-0.39

4. NUMERICAL EXAMPLES

4.1 Arch-type Truss Model

Maximum responses of a pin-jointed arch-type truss as shown in Fig. 3 are found for verification of the proposed method. The program called FEDEASLab [11] on MATLAB is used for inelastic static/dynamic response analysis. The arch is subjected to horizontal excitation. The lower columns also consist of pin-jointed trusses. See Ref. [12] for details of the model. The design response spectrum is multiplied by the factor 1.25. The damping modification factor κ is 0.33 assuming Type-C in ATC-40, which does not have enough energy dissipation property. The initial damping ratio is 2% for the 1st mode. The total strain energy defined in Ref. [9] is $3.22 \text{ kN} \cdot \text{m}$, and the ratios of the modes are 72% for the first, and 26% for the third. Therefore, we consider the first and third modes in the following

Load coefficients are computed for various phase differences. Since we consider only two modes, the phase of the first mode can be fixed as $\theta_1 = 0$. Eight sets of load coefficients are found for phase differences $\theta_3 = 0, \pi/8, \dots, 7\pi/8$ for maximizing $r_{10}(t) + r_{30}(t)$, which are denoted by Pattern 1 (P1-1, ..., P1-8) as listed in Table 1. Eight sets are also found for maximizing $r_{10}(t) - r_{30}(t)$, which are denoted by Pattern 2 (P2-1, ..., P2-8) as listed in Table 2.

The maximum responses are found for the displacements d_1, \dots, d_5 and the reaction forces F_1 , and F_2 indicated in Fig. 3. As is seen from the mode shape in Fig. 4, the horizontal components of modes 1 and 3 have the same sign; however, the vertical components have different signs. Therefore, Pattern 1 is used for d_1, d_2, d_3 , and F_1 , while Pattern 2 is used for d_4, d_5 , and F_2 .

The histories of the mode components of displacements are defined as $D_n(t) = \mathbf{\Phi}_n^T \mathbf{Mu}(t) / \Gamma_n$. The result for a spectrum-compatible wave is plotted in Fig. 5. It has been observed that the components of higher modes increase after a member yields. It has also been confirmed that the time at which the response takes the maximum is different for each component, which verifies the necessity of considering several phase differences between the dominant modes.

The inelastic responses are estimated using the load patterns in Tables 1 and 2. The results are shown in Fig. 6 in comparison to the mean-maximum values by the time-history analysis for spectrum-compatible 10 seismic motions. As is seen, the inelastic responses have been estimated with good accuracy. The relation of capacity and demand diagrams for Pattern P2-8 is plotted in Fig. 7, where the demand diagram can be approximated by a bilinear relation, and the yield point (D_y, A_y) is defined with the yielding of a member. The predicted ratio of

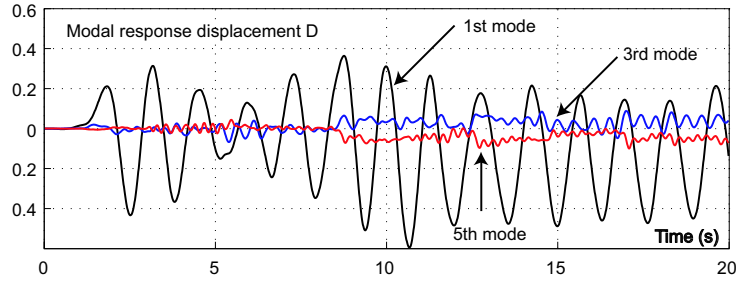


Fig.5. Time histories of modal responses.

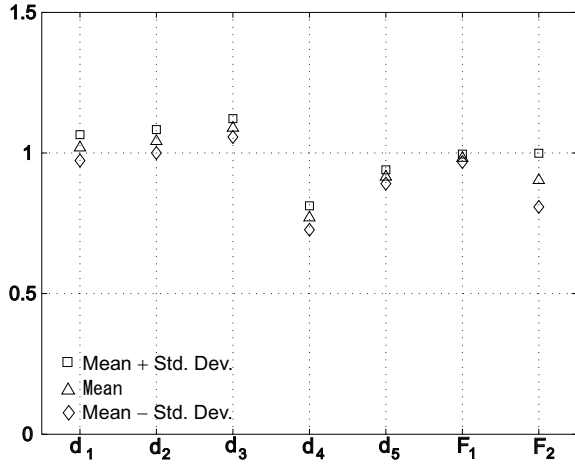


Fig.6. Ratios of mean and mean±standard deviation of the inelastic responses obtained by pushover analysis to the mean value by dynamic analyses.

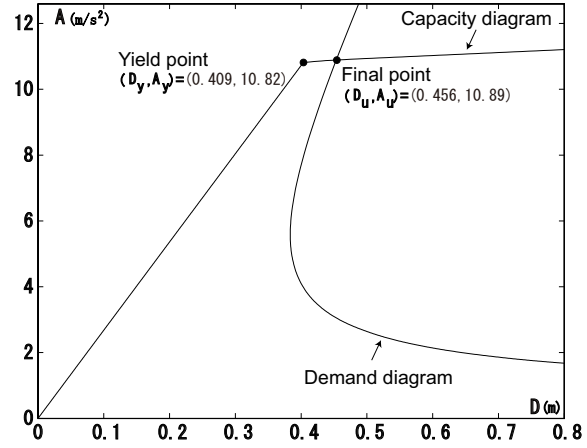


Fig.7. Capacity and demand diagrams for load pattern P2-8.

displacements to the mean value of time-history analysis for d_1 , d_2 , d_3 , d_4 , and d_5 are 1.55, 1.56, 1.56, 1.61, and 1.45, respectively, whereas the ratio of the forces F_1 and F_2 are 0.63 and 0.43, respectively. Therefore, the representative acceleration will be underestimated if the effect of modes higher than 4th is not incorporated.

The number of yielded members and the plasticity ratio by time-history analysis are 20 and about 2.0, respectively, for each motion. For the static analysis, the number of yielded members is 4 for Pattern P1, and 6 for Pattern P2, and the plasticity ratio is about 1.5 for both patterns. The member connecting the roof and the column first yields for Pattern P1, which results in drastic degradation of the horizontal load-carrying capacity. However, a chord member in the region between nodes A and B first yields for Pattern P2, which results in the deformation without yielding of the column.

4.2 Building Frame Model

Consider next a 3-story 3-dimensional frame model as shown in Fig. 8. OpenSees [13] is used for analysis. The cross-sectional dimensions are: Column: B-500×500×22, Beam (x -dir.): H-600×200×9×16, Beam (y -dir.): H-600×200×12×19. The elastic modulus is 2.05×10^8 kN/m², and the yield stress is 2.35×10^5 kN/m². The thickness of slab in each floor is 0.2 m, and the mass density is 2.3×10^3 kg/m³. The first and second modes dominate in x - and y -directional motions, respectively. These modes are used for evaluation of the axial force of the corner

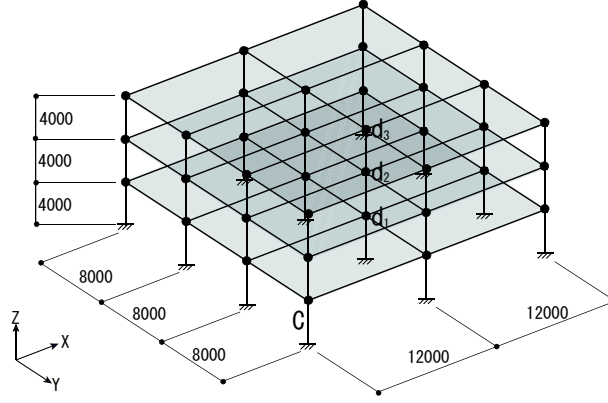


Fig.8. A 3-story 3-dimensional frame model.

Table 3. Load coefficients α_n .

	P1	P2	P3	P4	P5	P6	P7	P8
α_1	1.00	1.00	1.00	0.99	0.98	0.93	0.86	0.78
α_2	1.00	1.00	0.99	0.98	0.97	0.91	0.81	0.67

Table 4. Maximum axial forces F for each pattern and its ratio to the mean value $F_{THA} = 1057$ kN by time-history analysis.

	P1	P2	P3	P4	P5	P6	P7	P8
F (kN)	1172	1172	1168	1170	1169	1167	1158	1137
F/F_{THA}	1.109	1.109	1.105	1.107	1.106	1.104	1.095	1.075

column C in Fig. 8 against the seismic motions corresponding to the design responses spectrum scaled by 5.0.

The load coefficients for maximizing $r_{10}(t) + r_{20}(t)$ are obtained as shown in Table 3. The responses in x - and y -directions are denoted by the subscripts x and y , respectively, and D_x , D_y , A_x , and A_y can be computed by pushover analysis for the static load as a combination of the first and second modes. Then the representative displacement and acceleration are obtained as

$$D^i = \sqrt{(D_x^i)^2 + (D_y^i)^2}, \quad A^i = \sqrt{(A_x^i)^2 + (A_y^i)^2} \quad (12)$$

The demand diagram is also defined as

$$A^R = \sqrt{(A_x^R)^2 + (A_y^R)^2} \quad (13)$$

Table 4 shows the comparison between the results by pushover analysis and time-history analysis. As can be seen, the inelastic responses are estimated within the accuracy of $\pm 10\%$ of the dynamic responses. The ratio of the standard deviation to the mean value is 0.00857 for pushover analysis, and 0.03652 for time-history analyses; i.e., the variation of maximum responses could not be estimated in this case by the pushover analysis. The maximum axial forces obtained only by the 1st and 2nd modes, respectively, are 690 kN and 918 kN, which underestimate the results.

5. CONCLUSIONS

A new procedure has been proposed for predicting the maximum inelastic responses of spatial frames subjected to seismic motions. Since more than one mode dominate in the seismic re-

sponses, the peak modal responses are computed making use of different phase angles for the sinusoidal modal responses to define several patterns of equivalent static loads as a weighted sum of the modal loads. The equivalent loads are incorporated into the capacity spectrum method, which has been extended to account for higher modes, to estimate the peak response by a series of pushover analyses. New definitions have been presented for representative displacement and acceleration for spatial frames considering higher modes, for which the base shear and roof displacement that are used for regular building frames cannot be used.

It has been shown in the numerical studies of a long-span arch model that the proposed method can accurately estimate the maximum inelastic responses within $\pm 10\%$ of the mean values obtained by time-history analyses for the spectrum-compatible seismic motions. The deviations of the dynamic responses can also be estimated by using the proposed method with successive static pushover analyses. It has also been shown that the maximum axial force of the column at the corner of a three-dimensional building frame subjected to multi-directional motions can also be predicted with good accuracy using the proposed method.

REFERENCES

1. P. Fajfar. The N2 method for the seismic damage analysis of RC buildings. *Earthquake Eng. Struct. Dyn.*, 25(1):31–46, 1996.
2. B. Gupta and S. K. Kunnath. Adaptive spectra-based pushover procedure for seismic evaluation of structures. *Earthquake Spectra*, 16(2):367–392, 2000.
3. A. K. Chopra and R. K. Goel. A modal pushover analysis procedure for estimating seismic demands for buildings. 31:561–582, 2002.
4. H. G. Park, T. Eom, and H. Lee. Factored modal combination for evaluation of earthquake load profiles. *J. Struct. Engng., ASCE*, 133(7):956–968, 2007.
5. S. K. Kunnath. Identification of modal combinations for nonlinear static analysis of building structures. *Computer-Aided Civil and Infrastructure Eng.*, 19:246–259, 2004.
6. S. Nakazawa, S. Kato, T. Yoshino, and K. Oda. Study on seismic response estimation based on pushover analysis for membrane structure supported by substructure. In *Proc. IASS Symposium*, Bucharest, 2005.
7. S. Kato, S. Nakazawa, and K. Saito. Two-modes pushover analysis for reticular domes for use of performance based design for estimating responses to severe earthquakes. In *Proc. IASS Symposium*, Bucharest, 2005.
8. A. K. Chopra and R. K. Goel, Capacity-demand-diagram methods for estimating seismic deformation of inelastic structures: SDF systems, Report No. PEER-1999/02. PEERC, Univ. California, Berkeley, CA, 1999.
9. S. Kato, S. Nakazawa, and K. Saito. Estimation of static seismic loads for latticed domes supported by substructure frames with braces deteriorated due to buckling. *J. Int. Assoc. Shell and Spatial Struct.*, 48(2):71–86, 2007.
10. Applied Technology Council. *Seismic evaluation and retrofit of concrete buildings, Report ATC 40*, 1996.
11. F. C. Filippou and M. Constantinides. Fedeaslab getting started guide and simulation examples. Tech. Report NEESgrid-2004-22, Dept. of Civil and Env. Eng., UCB, 2004.
12. A. Uchida, M. Ohsaki and J. Y. Zhang. Prediction of inelastic seismic responses of spatial structures by static analysis with higher modes. *J. Struct. Eng.*, 55B, 2009. (in Japanese)
13. S. Mazzoni, F. McKenna and G. L. Fenves, Getting Started with OpenSees, Tech. Report NEESgrid-2004-21, Dept. of Civil and Environmental Eng., UCB, 2004.